

# Dosimetric comparison of large field widths in helical tomotherapy for intracranial stereotactic radiosurgery

A. Watcharawipha<sup>1,2</sup>, I. Chitapanarux<sup>1,2,3\*</sup>, B. Jia-Mahasap<sup>1,2</sup>

<sup>1</sup>Division of Radiation Oncology, Faculty of Medicine, Chiang Mai University, Chiang Mai, Thailand

<sup>2</sup>Northern Thai Research Group of Radiation Oncology (NTRG-RO), Faculty of Medicine, Chiang Mai University, Chiang Mai, Thailand

<sup>3</sup>Chiang Mai Cancer Registry, Maharaj Nakorn Chiang Mai Hospital, Faculty of Medicine, Chiang Mai University, Chiang Mai, Thailand

## ABSTRACT

### ► Original article

#### \*Corresponding author:

Imjai Chitapanarux, M.D.,

E-mail: [imjai@hotmail.com](mailto:imjai@hotmail.com)

Received: March 2021

Final revised: March 2022

Accepted: March 2022

Int. J. Radiat. Res., July 2022;  
20(3): 701-707

DOI: 10.52547/ijrr.20.3.26

**Keywords:** Dynamic jaws, field width, stereotactic radiosurgery, helical tomotherapy.

**Background:** The Helical Tomotherapy (HT) technique has been introduced for use in Stereotactic Radiosurgery (SRS). Previously, the smallest field width (FW) has been recommended for optimum results, which would require a long beam-on time (BoT). The uncertainty of the intrafraction could be maximized during the delivery by this BoT. This study then investigated the plan qualities and dosimetric parameters among different FWs and treatment modes. **Materials and Methods:** Fifteen patients previously treated by the HT technique with fixed-FW 10 mm (FW10f) were selected. The treatment planning systems of TomoTherapy involved other plans that employed fixed-FW 25 mm (FW25f) and dynamic-FW 25 mm (FW25d). The plan quality indexes and the dosimetric parameters of the large FWs (FW 25 mm) were compared according to the FW10f benchmark and then analyzed by relevant statistics. **Results:** The plan quality indexes and the dosimetric parameters revealed no significant differences between FW10f and FW25d. Accordingly, FW25f revealed a significant difference in the FW10f values in some indexed parameters. The maximum dose on the right optic nerves and the value of the integral dose revealed a significant difference between FW10f and FW25f. The BoT of the FW10f presented the longest treatment time when compared with the other FWs. **Conclusion:** The outcomes of this investigation clearly ensure that the performance of FW25d is comparable with that of FW10f in terms of the plan qualities and the dosimetric parameters. Notably, the short BoT of this FW might benefit the minimization that is associated with intrafraction uncertainty.

## INTRODUCTION

Stereotactic radiosurgery (SRS) is widely used in neurosurgery when open surgery cannot be used to treat lesions. A single dose of radiation, as well as fractionated SRS, can result in a high radiation dose being delivered to the target. This is because excessive amounts of beam directions in the non-coplanar plans can be primarily administered in the SRS technique. The current SRS delivery system is known to use the Gamma Knife<sup>(1-3)</sup>, Linear accelerator (LINAC)<sup>(4-6)</sup>, CyberKnife®<sup>(1, 3, 7)</sup>, etc. In this regard, TomoTherapy® is recognized as a LINAC-based SRS system<sup>(2, 5, 6, 8, 9)</sup>. Although treatment plans are restricted by the treatment planes, the plan quality of the Helical Tomotherapy (HT) technique must meet the requirements of the SRS technique<sup>(10)</sup>.

Holmes *et al.*<sup>(10)</sup> introduced the HT technique in the intracranial and extracranial SRS, while TomoTherapy was developed for the general delivery of the IMRT technique<sup>(8)</sup>. The HT technique is known

to provide a high degree of accuracy for both SRS and the Stereotactic Body Radiotherapy (SBRT) because of the built-in megavoltage imaging system<sup>(8)</sup>. Soisson *et al.*<sup>(11)</sup> proposed guidelines for intracranial SRS treatment planning that can be used with the HT technique. Various virtual structures have been created in the treatment plans to provide a high dose of radiation to the target and a rapid fall-off of the dose to surrounding tissue. The recommended plan parameters include the pitches, the modulation factors (MF), the dose constraints, and the field width (FW). The smallest FW value (fixed-FW 10 mm) has been recommended for dose delivery. This FW resulted in a longer treatment time because the beam-on time (BoT) of the TomoTherapy was dependent upon the size of the FW<sup>(12)</sup>. On the other hand, the degree of intrafraction uncertainty may be maximized over an extended period of BoT<sup>(13)</sup>. TomoTherapy provided a mode of the dynamic jaws on the large FW that appeared as an advantage in terms of radiation dose reduction, as has been illustrated in

figure 1. In contrast to the static FW shown in figure 1a, half of the FW was opened when the target was accessed as is shown in figure 1b. In the event that the large FW of the TomoTherapy is employed in the SRS, the patient would receive the benefit of not only dose reduction but also less BoT. Saw *et al.* <sup>(14)</sup> implemented the SRS with the HT technique in a clinical trial. The dynamic-FW 25 mm was employed in this study but was not mentioned in a dosimetric comparison involving different FWs. Murai *et al.* <sup>(8)</sup> compared the plan quality indexes and dosimetric parameters of different FWs. A dosimetric comparison was made that involved simulated targets for three different FWs, but only two different FWs were employed in the clinical situation. A lack of any other FW comparisons in a clinical situation may not provide researchers with sufficient information on FW performance. Agostinelli *et al.* <sup>(9)</sup> compared the plan quality indexes and dosimetric parameters of different FWs in the HT technique. The comparison, however, focused only on the fixed-FW modes between 10 mm and 25 mm.

Although TomoTherapy was employed on SRS, the smallest FW (fixed-FW 10 mm) of the delivery was widely utilized <sup>(2, 6, 11)</sup>. The treatment time was particularly increased during radiation delivery by employing the smallest FW <sup>(12)</sup>. By utilizing a large FW (FW 25 mm), the plan qualities and organ doses were included in the interrogations. This study then investigated the plan qualities and dosimetric parameters involved with intracranial SRS by utilizing large FWs (FW 25 mm). This investigation allowed researchers to observe the capability of the large FWs in not only the dynamic-FW mode but also in the fixed-FW mode. The resulting statistics were considered along with 95% confidence interval to analyze the results by utilizing fixed-FW 10 mm, fixed-FW 25 mm, and dynamic-FW 25 mm. A comparison of the performance focused not only on the plan qualities and dosimetric parameters but also on the

integral dose (ID) and BoT by the fixed-FW 10 mm benchmark.

## MATERIALS AND METHODS

### Ethical statement

This investigation involved a retrospective study. Each patient was randomly recruited based on relevant information acquired during the period from June 2019 to May 2020. The protocol for this study was approved of by the Ethics Committee of Chiang Mai University on 9 June, 2020. (Study code: RAD-2563-07365).

### Data preparation

Fifteen patients with single or multiple brain metastases were selected to be included in this study. In this experiment, 53.3% of the samples were male and 46.7% were female. The ages of the subjects in this group were established to be within the range of  $68.8 \pm 10.6$  years old according to mean  $\pm$  standard deviation values (mean  $\pm$  SD). Other details related to patient characteristics have been described in table 1. A computed tomography simulator (SOMATOM Definition AS, Siemens Healthineers, Forchheim, Germany) established the image set with the use of one mm of slice thickness. With regard to delineation of the target and organs at risk (OARs), the three-dimensional T1-weighted image set with contrast media (Gadolinium) was established by Magnetic Resonance Imaging Scanner (1.5 T SIGNA Horizon, GE Healthcare, WI, USA) and then registered on the image set of the computed tomography. The gross target volume (GTV) was delineated on each image set of the patient and expanded by 2 mm to the planning target volume (PTV). Other organs at risk were also identified that included the optic nerves, the optic chiasm, the brainstem, the eyes, and the whole brain.

Table 1. Patient characteristics and plan parameters of the treatment planning.

Case No.	PTV no.	Gender	Age	Dx	PTV (cc)	Treatment length (mm)	Maximum dose (Gy)	Prescribed dose (Gy)	Pitch	Modulation Factor
1	1	M	69	Ca lung	2.12	14.00	24.00	20.00	0.10	1.70
2	1	M	75	Ca lung	1.39	16.00	24.00	20.00	0.05	1.70
3	1	M	75	Ca lung	5.28	24.00	18.00	15.00	0.05	1.70
4	1	F	72	Ca lung	10.87	26.00	18.00	15.00	0.10	1.70
5	1	F	56	Ca breast	0.79	11.00	24.00	20.00	0.10	1.70
6	1	M	70	Ca lung	5.43	21.00	21.60	18.00	0.10	1.70
7	1	M	72	Ca lung	15.46	37.00	18.00	15.00	0.10	1.70
8	1	M	85	Ca lung	3.50	18.00	21.50	18.00	0.10	1.70
9	1	F	43	Ca lung	14.99	66.00	18.00	15.00	0.10	1.70
	2				0.50		24.00	20.00		
10	1	F	85	Ca lung	8.68	29.00	18.00	15.00	0.10	1.70
11	1	F	68	Ca breast	8.44	28.00	21.60	18.00	0.10	1.70
	2				0.76		24.00	20.00		
12	1	F	67	Ca lung	1.15	14.00	24.00	20.00	0.10	1.70
13	1	M	62	Ca rectum	13.29	41.00	18.00	15.00	0.10	1.70
	2				0.93		24.00	20.00		
14	1	F	61	Ca lung	1.98	18.00	21.60	18.00	0.10	1.70
15	1	M	72	Ca lung	4.03	22.00	21.60	18.00	0.10	1.70
Mean			68.8		5.53	28.94	21.31	17.78	0.09	1.70
SD			10.6		5.17	16.18	2.70	2.18	0.02	0.00

### Treatment planning

Treatment plans were created by utilizing the Hi-Art® version 5.1.4 (Accuray Inc., Sunnyvale, CA). The plans of the HT were performed on the image set of the patient in three scenarios that included fixed-FW 10 mm (FW10f), fixed-FW 25 mm (FW25f), and dynamic-FW 25 mm (FW25d). PTV was prescribed within a range of 15-20 Gy for a single fraction. The coverage of the prescribed dose was at least 99% of the PTV and 100% of the GTV. Plan parameters were set according to the recommendations of Soison *et al* <sup>(11)</sup>. The value of the pitch and the modulation factor (MF) were set at 0.05-0.10 and 1.7, respectively. The separation of the treatment plans was dependent upon the distance between each target in the longitudinal axis. The finest calculation grid was then used for both the fluence optimization and dose calculation steps. All samples were previously treated with FW10f of the HT technique of TomoTherapy (Accuray Inc., Sunnyvale, CA).

### Treatment planning evaluation

Various plan quality indexes were used to evaluate the performance between FW10f and each mode of the large FW. These indexes consisted of the homogeneity index (HI), the conformity index (CI), the conformity index at 50% of the prescribed dose (CI<sub>50</sub>), the gradient score index (GSI), and the integral dose (ID).

Homogeneity index (HI) was determined by  $D_{max}/D_{Rx}$ .  $D_{max}$  represents the maximum radiation dose, whereas  $D_{Rx}$  represents the prescribed radiation dose. The definition of this index differed from the International Commission on Radiation Units and Measurements <sup>(15)</sup> (ICRU) in accordance with consideration of the maximum dose.

Conformity index (CI) was expressed as  $CI = (PTV \times PIV)/TV_{PIV}^2$ . Accordingly,  $TV_{PIV}$  is the target volume that receives the prescribed isodose volume.  $PTV$  is the planning target volume.  $PIV$  is the prescribed isodose volume. The index was proposed by Paddrick <sup>(16)</sup> and is commonly used in the SRS/SRT technique.

Conformity index at 50% of the prescribed dose (CI<sub>50</sub>) was employed to determine the dose outside of the target. The index was determined by  $PIV_{50\%,Rx}/PIV$ , where  $PIV_{50\%,Rx}$  is representative of the volume at 50% of the prescribed isodose dose.

Gradient Score Index <sup>(17)</sup> (GSI) is another index that observes the dose outside of the target that is also present in the distance. This index determines the gradient distance between the prescribed dose ( $R_{eff}$ ) and 50% of the prescribed dose ( $R_{eff,50\%Rx}$ ) by  $100 - (100 \times ([R_{eff,50\%Rx} - R_{eff}] - 0.03))$ .  $R_{eff}$  and  $R_{eff,50\%}$  represent the effective radius (cm) and are determined by  $\sqrt[3]{3V/4\pi}$  and  $\sqrt[3]{3V_{50\%,Rx}/4\pi}$ , respectively.  $V$  and  $V_{50\%,Rx}$  represent the isodose volume in the cc of  $PIV$  and  $PIV_{50\%,Rx}$ , respectively. The gradient distance ( $R_{eff,distance}$ ) is determined by the difference in

the distance between  $R_{eff}$  and  $R_{eff,50\%}$ . Importantly, this index should not be larger than one centimeter.

Integral dose (ID) is used to determine the exceeded dose in the patient. ID is normally used to evaluate the low dose in the medium, especially for the IMRT technique. The index is determined by  $D_{mean} \times V$  where the unit is Gy.L.,  $D_{mean}$  is the mean dose (Gy), and  $V$  is the object volume (L).

The dosimetric parameter of the organs at risk was also used to evaluate the performance of the different FWs. The major normal organs were observed not only in terms of the  $D_{max}$  values on the eyes, the optic nerves, the optic chiasm, and the brainstem, but also in terms of the absolute volume of the whole brain that received a dose of 5 Gy ( $V_{5Gy}$ ).

### Statistical analysis

The SPSS (International Business Machine Corp, NY, USA) version 25 was used to analyze the relevant indexes and the dosimetric parameters. The results were then analyzed by one-way ANOVA with 95% confidence interval.

## RESULTS

The details of the planning parameters are shown in table 1. The case involved a single lesion value of 80% of the samples, whereas the value for multiple lesions was 20%. The multiple lesions of each case included a lesion value that did not exceed two lesions. The size of the PTV and the distance of the treatment length were  $5.53 \pm 5.17$  cc and  $28.94 \pm 16.18$  mm established by mean  $\pm$  SD values, respectively. The mean of dose prescription was  $17.78 \pm 2.78$  Gy. The treatment plan was accepted at 83.43% of the  $D_{max}$ . The value of the pitch was set at  $0.09 \pm 0.02$ , whereas the MF was 1.70.

Table 2 demonstrates the plan quality indexes and the dosimetric parameters including the BoT. The results reveal no significant differences in the values of the minimum dose ( $D_{min}$ ), the maximum dose ( $D_{max}$ ), the HI, the CI, and the CI<sub>50</sub> between the FW10f and each jaw mode of the FW25. The FW25f revealed a significant difference in the level of the GSI ( $p < 0.01$ ) and the distance of the  $R_{eff,distance}$  ( $p < 0.01$ ). The results of FW25f demonstrated a lower level of the GSI and a higher distance of the  $R_{eff,distance}$  than for FW10f. In the case of OARs, the statistical analysis presented no significant differences in the  $D_{max}$  values for both eyes, the brainstem, the optic chiasm, the left optic nerve, and the  $V_{5Gy}$  of the whole brain between the FW10f and each jaw mode of the FW25. A significant difference was shown in terms of the dose of the right optic nerve ( $p = 0.037$ ) and the value of the ID ( $p = 0.049$ ) between FW10f and FW25f. Finally, the BoT was analyzed. This result showed a significant difference between FW10f and the other FW25s. Accordingly, the BoT of the FW10f was much higher

than those of FW25f ( $p < 0.01$ ) and FW25d ( $p < 0.01$ ). Figure 2 demonstrates an example of the dose distribution in the transverse, the sagittal, and the coronal planes with the use of three different FWs. The PTV received 80% of 24 Gy in a single fraction. The figure

clearly illustrates a larger dose volume for the FW25f plan (figure 2b) than for either the FW10f plan (figure 2a) or the FW25d plan (figure 2c) in terms of the craniocaudal direction.

**Table 2.** Mean and Standard deviation (Mean  $\pm$  SD) of the plan quality indexes, dosimetric parameters and BoT.

Quality index	FW10f	FW25f	FW25d
Dmin (Gy)	17.50 $\pm$ 2.20	17.52 $\pm$ 2.34	17.54 $\pm$ 2.40
Dmax (Gy)	21.43 $\pm$ 2.48	21.38 $\pm$ 2.48	21.36 $\pm$ 2.47
HI	1.21 $\pm$ 0.02	1.20 $\pm$ 0.03	1.20 $\pm$ 0.03
CI	1.45 $\pm$ 0.33	1.53 $\pm$ 0.42	1.49 $\pm$ 0.37
CI <sub>50</sub>	8.69 $\pm$ 4.11	12.09 $\pm$ 6.83	9.60 $\pm$ 5.55
GSI	50.32 $\pm$ 10.94	<b>32.96 <math>\pm</math> 11.44</b> ( $p < 0.01$ )	45.21 $\pm$ 14.23
R <sub>eff,distance</sub> (cm)	0.80 $\pm$ 0.11	<b>0.97 <math>\pm</math> 0.11</b> ( $p < 0.01$ )	0.85 $\pm$ 0.14
<b>Organ at Risk</b>			
Eye (Gy) Right	0.99 $\pm$ 1.11	1.87 $\pm$ 3.18	0.92 $\pm$ 1.07
Left	0.68 $\pm$ 0.74	0.83 $\pm$ 0.82	0.66 $\pm$ 0.74
Brainstem (Gy)	1.97 $\pm$ 2.34	2.26 $\pm$ 2.37	2.10 $\pm$ 2.32
Optic chiasm (Gy)	1.34 $\pm$ 1.92	2.06 $\pm$ 3.29	1.36 $\pm$ 2.04
Optic Nerve (Gy) Right	0.87 $\pm$ 1.09	<b>2.14 <math>\pm</math> 3.44</b> ( $p = 0.037$ )	0.83 $\pm$ 1.06
Left	0.63 $\pm$ 0.78	0.92 $\pm$ 0.96	0.62 $\pm$ 0.79
V <sub>5Gy</sub> of Whole brain (cc)	98.38 $\pm$ 61.52	132.54 $\pm$ 79.88	109.68 $\pm$ 78.73
ID (Gy×L)	2.84 $\pm$ 1.24	<b>3.76 <math>\pm</math> 1.44</b> ( $p = 0.049$ )	3.04 $\pm$ 1.42
Beam-on time (min)	16.61 $\pm$ 4.35	<b>8.79 <math>\pm</math> 1.59</b> ( $p < 0.01$ )	<b>9.29 <math>\pm</math> 1.50</b> ( $p < 0.01$ )

\*Bold letter is the significant difference ( $p < 0.05$ )

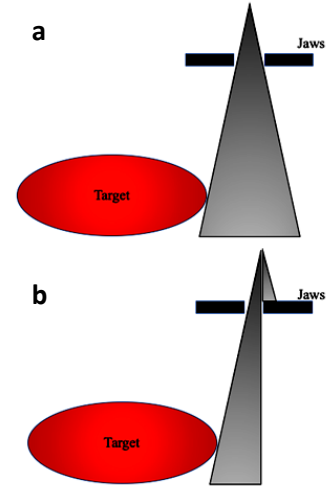


**Figure 1.** Schematic diagram of the static field width (a) and the dynamic field width (b) in the Tomotherapy.

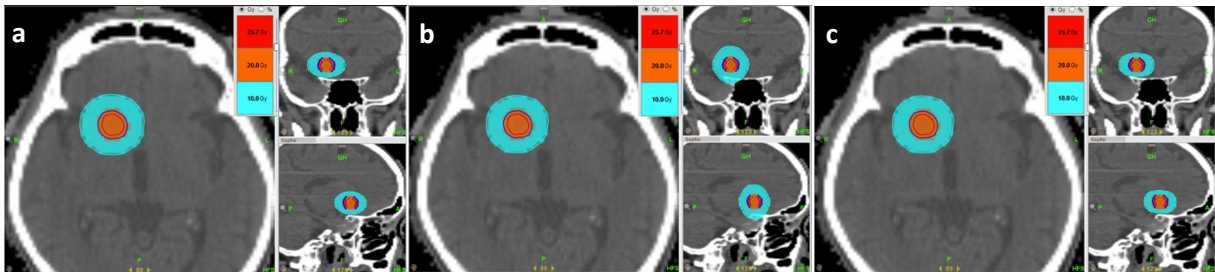


**Figure 2.** Example of the dose distribution in the transverse, sagittal and coronal plane by utilizing the fixed-FW 10mm (a), the fixed-FW 25mm (b) and the dynamic-FW 25mm (c). The GTV and the PTV are presented in the color of red and blue, respectively. The color wash of orange is the dose of 20 Gy whereas the turquoise is 10 Gy.

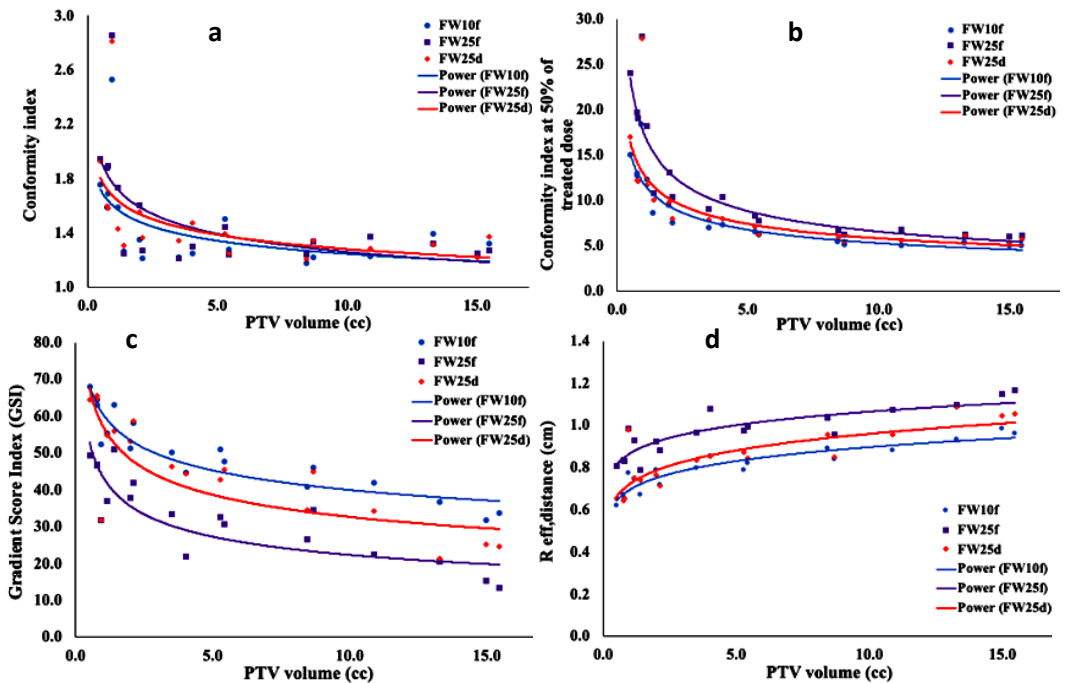


**Figure 3.** Plots and curve fittings between the PTV volume and the CI (a), CI<sub>50</sub> (b), the GSI (c), and the R<sub>eff,distance</sub> (d). The results and curves of the fixed-FW 10mm, the fixed-FW 25mm and the dynamic-FW 25mm present in the color of blue, purple and red, respectively.

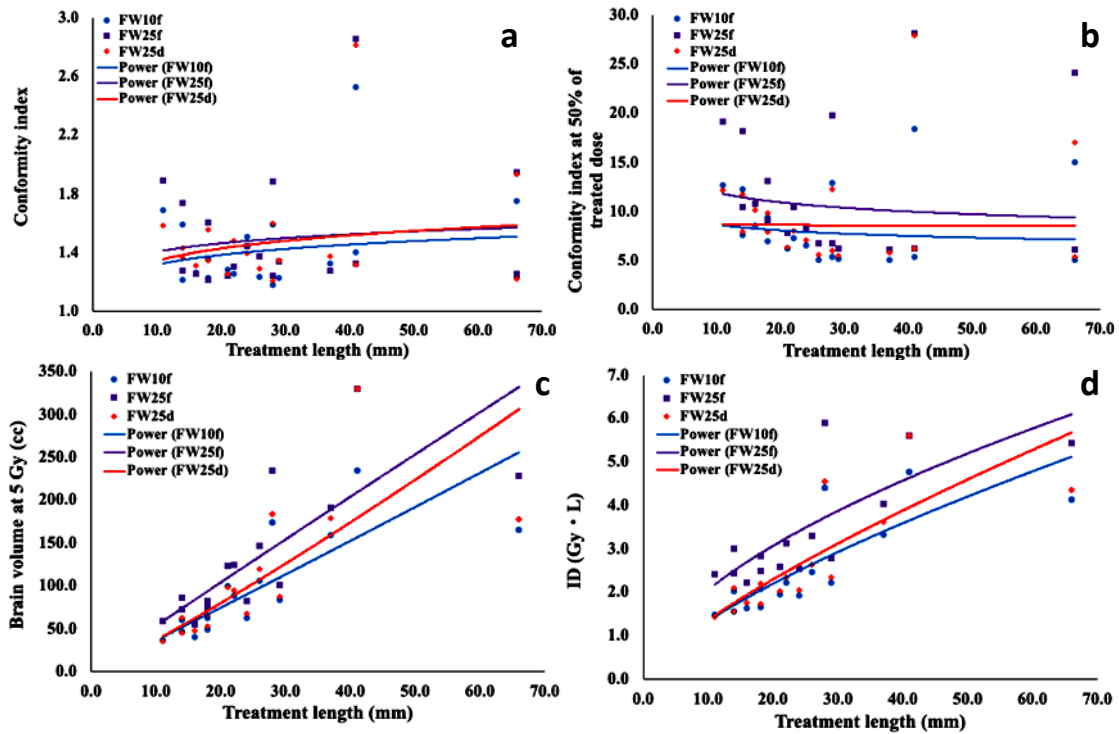


**Figure 4.** Plots and curve fittings between the treatment lengths and the CI (a), the CI50 (b), the brain volume at 5 Gy (c) and the ID (d). The results and curves of the fixed-FW 10mm, the fixed-FW 25mm and the dynamic-FW 25mm present in the color of blue, purple, and red, respectively.

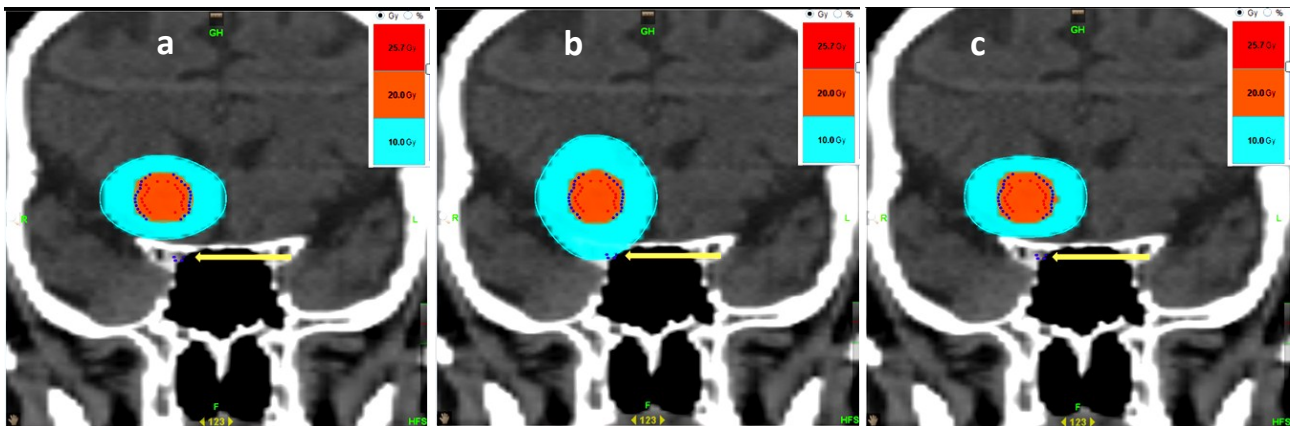


**Figure 5.** Example of the dose distribution impacted on the right optic nerve (purple dots) in the coronal plans. The plans of this case were employed by the fixed-FW 10mm (a), the fixed-FW 25mm (b) and the dynamic-FW 25mm (c). The GTV and the PTV are presented in the color of red and blue, respectively. The color wash of orange is the dose of 20 Gy whereas the turquoise is 10 Gy.

### DISCUSSION

This study focused on the applicable large FWs of the HT for SRS. Various plan quality indexes and dosimetric parameters were used to analyze the performance of each pair of different FWs. In terms of the plan qualities, the results revealed no significant differences in comparisons made between FW10f and FW25d, which was in agreement with the outcomes of a study conducted by Murai *et al.* (8). The value of the HI revealed a significant difference among the different FWs on the simulated target, which was not observed in the clinical situation of their study. In this study, the values were only parallel in the clinical situation of their work. The dose gradient is one of

the important parameters in the SRS technique. This value was presented in terms of the GSI and the  $R_{eff,distance}$ . For the GSI in this study, the value of the FW25f revealed a parallel result with the work of Agostinelli *et al.* (9). This value was presented as a low level of GSI for FW25f when compared with FW10f. This study found that the GSI value of FW10f was lower than what was reported in their study because of the size of the PTV. The smallest FW was employed to the limited size of the PTV, whereas this study investigated all sizes of the PTV with the same FW. The  $R_{eff,distance}$  of this study, however, revealed a value that was less than 10 mm according to the mean value. This would suggest that both modes of the large FWs are applicable for SRS, although the FW 25

mm is not recommended.

In determining the size of the PTV, various plan quality indexes were plotted against the size of the PTV. Figure 3 demonstrates the fitting curves when using the power function between the PTV volume and the value of the CI (figure 3a), the  $CI_{50}$  (figure 3b), the GSI (figure 3c), and the  $R_{eff,distance}$  (figure 3d). Figures 3a and b show a decrease in the CI and  $CI_{50}$  values, respectively, while the volume of the PTV was found to have increased. This trend appears to be in agreement with the work of Li *et al.* (18) who investigated the plan quality metric in intracranial SRS by utilizing Ring-based and C arm-based LINAC. In cases involving the GSI and the  $R_{eff,distance}$ , figures 3c and d show a decreased level of GSI and an increased distance of  $R_{eff,distance}$  versus an increased volume of PTV. These results agree with the outcomes of the work of Agostinelli *et al.* (9) and Yaparpalvi *et al.* (19). This would indicate that the volume of the PTV has to be considered in the SRS technique by utilizing all machine modalities. The length of the treatment is not represented by the volume of the PTV. Resolution of this issue would require further consideration, particularly in terms of what is being delivered by TomoTherapy. The treatment length (mm) was measured and then fitted to the curves using the power function against the values of the CI and the  $CI_{50}$  as is shown in figures 4a and b, respectively. Figure 4a shows that the value of CI is slightly increased when the length was increased. In contrast to  $CI_{50}$ , the value dose did not depend on the treatment length. This would indicate that the exceeded dose occurred along the target but not at the two ends.

In terms of the dosimetric parameters, various OARs were used to evaluate the performance between each pair of the different FWs. This study focused on diseases involving brain metastasis where the brain volume is considered a major normal organ. The results showed that the  $V_{5Gy}$  values of the whole brain were not significantly different in comparisons made between each pair of the different FWs. This result is in contrast to the outcomes of a simulated target investigation conducted by Murai *et al.* (8). A volume of low dose was observed along with the fitting curve against the  $V_{5Gy}$  value of the whole brain and the value of ID, all of which are shown in figures 4c and d, respectively. The curves indicate that the increment of the length and brain volume as well as the ID are linear. By introducing the dynamic jaw, this mode of TomoTherapy can benefit normal organ sparing. In a study conducted by Zhang *et al.* (20), a decrease in dose was observed in terms of the superior/inferior area of the target in the nasopharyngeal carcinoma when utilizing this mode. The results of this study are in agreement with the outcomes of that study as has been indicated by the dose delivered to the right optic nerve. Figure 5 illustrates the dose distribution that was performed by FW10f, FW25f, and FW25d in the coronal plane.

These outcomes reveal that the right optic nerve received a low dose on the dynamic mode when the FW25 was employed. The fixed-FW mode of FW25mm provided a high dose on the adjacent superior/inferior organs, however, this FW can be applicable with this consideration in mind (9).

Remarkably, the BoT was the most impacted parameter when different FWs were employed. The results indicate a large reduction in treatment time when a large FW was used in the plan. This study produced results that are in agreement with those of the studies conducted by Murai *et al.* (8) and Zhang *et al.* (20). Therefore, it was determined that a reduction in BoT could minimize the chances of an occurrence of intrafraction uncertainty that would result from patient movement.

## CONCLUSION

This study investigated the different FWs performance values of TomoTherapy. The results clearly ensure that the performance of the dynamic-FW 25 mm is comparable to that of the fixed-FW 10 mm in the plan qualities and dosimetric parameters. The short beam-on time of this FW might be beneficial in terms of intrafraction uncertainty. Finally, it has been concluded that the applications of the fixed-FW 25 mm should be available for SRS/SRT with the consideration.

## ACKNOWLEDGEMENT

*This research is no acknowledgement.*

**Conflicts of Interest:** The authors declare no conflict of interest.

**Ethical statement:** This investigation involved a retrospective study. Each patient was randomly recruited based on relevant information acquired during the period from June 2019 to May 2020. The protocol for this study was approved of by the Ethics Committee of Chiang Mai University on 9 June, 2020. (Study code: RAD-2563-07365).

**Funding:** This research received no external funding.

**Authorship:** Anirut Watcharawipha (AW), Imjai Chitapanarux (IC) and Bongkot Jia-Mahasap (BJ) AW and IC: Conception and design; AW, IC and BJ: Analysis and interpretation of data; AW, BJ: Drafting the article; AW, IC and BJ: Revising it critically for important intellectual content; IC: Final approval of the version to be published.

## REFERENCES

1. Sio TT, Jang S, Lee SW, Curran B, Pyakuryal AP, Sternick ES (2014) Comparing Gamma Knife and CyberKnife in patients with brain metastases. *J Appl Clin Med Phys*, 15(1): 14–26.
2. Mori Y, Nakazawa H, Hashizume C, Tsugawa T, Murai T (2019) Dosimetric comparison of hypofractionated stereotactic radiotherapy by three different modalities for benign skull base tumors

- adjacent to functioning optic pathways. *Int J Radiat Res*, **17**(4): 519-530.
3. Wowra B, Muacevic A, Tonn JC (2009) Quality of radiosurgery for single brain metastases with respect to treatment technology: a matched-pair analysis. *J Neurooncol*, **94**(1): 69-77.
  4. Shao Y, Chen H, Wang H, Cheng Y, Zhu Z, Zhuo W, et al. (2022) Target dose accuracy of single-isocenter stereotactic body radiation therapy for multiple lung lesions. *Int J Radiat Res*, **20**(1): 241-244.
  5. Yip HY, Mui WLA, Lee JWY, Fung WWK, Chan JMT, Chiu G, et al. (2013) Evaluation of radiosurgery techniques-cone-based linac radiosurgery vs tomotherapy-based radiosurgery. *Med Dosim*, **38**(2): 184-189.
  6. Lee TF, Chao PJ, Wang CY, Lan JH, Huang YJ, Hsu HC, et al. (2011) Dosimetric comparison of helical tomotherapy and dynamic conformal arc therapy in stereotactic radiosurgery for vestibular schwannomas. *Med Dosim*, **36**(1): 62-70.
  7. Bijina T, Ganesh K, Subbulakshmi B, Pichandi A (2020) Dosimetric comparison of single and double collimator stereotactic body radiotherapy plans using Cyber Knife for carcinoma prostate. *Int J Radiat Res*, **18**(2): 209-217.
  8. Murai T, Hayashi A, Manabe Y, Sugie C, Takaoka T, Yanagi T, et al. (2016) Efficacy of stereotactic radiotherapy for brain metastases using dynamic jaws technology in the helical tomotherapy system. *Br J Radiol*, **89**(1066): 20160374.
  9. Agostinelli S, Garelli S, Gusinu M, Zeverino M, Cavagnetto F, Pupillo F, et al. (2018) Dosimetric analysis of Tomotherapy-based intracranial stereotactic radiosurgery of brain metastasis. *Phys Med*, **52**: 48-55.
  10. Holmes TW, Hudes R, Dziuba S, Kazi A, Hall M, Dawson D (2008) Stereotactic image-guided intensity modulated radiotherapy using the HI-ART II helical tomotherapy system. *Med Dosim*, **33**(2): 135-148.
  11. Soisson ET, Hoban PW, Kammeyer T, Kapatoes JM, Westerly DC, Basavatia A, et al. (2011) A technique for stereotactic radiosurgery treatment planning with helical tomotherapy. *Med Dosim*, **36**(1): 46-56.
  12. Yawichai K, Chitapanarux I, Wanwilairat S (2016) Helical tomotherapy optimized planning parameters for nasopharyngeal cancer. *J Phys Conf Ser*, **694**: 012002.
  13. Mangesius J, Seppi T, Weigel R, Arnold CR, Vasilijevic D, Goebel G, et al. (2019) Intrafractional 6D head movement increases with time of mask fixation during stereotactic intracranial RT-sessions. *Radiat Oncol*, **14**(1): 231.
  14. Saw CB, Gillette C, Peters CA, Koutcher L (2018) Clinical implementation of radiosurgery using the Helical Tomotherapy unit. *Med Dosim*, **43**(3): 284-290.
  15. Hodapp N (2012) The ICRU Report 83: prescribing, recording and reporting photon-beam intensity-modulated radiation therapy (IMRT). *Strahlenther Onkol*, **188**(1): 97-99.
  16. Paddick I (2000) A simple scoring ratio to index the conformity of radiosurgical treatment plans. *Technical note. J Neurosurg*, **93**(3): 219-222.
  17. Wagner TH, Bova FJ, Friedman WA, Buatti JM, Bouchet LG, Meeks SL (2003) A simple and reliable index for scoring rival stereotactic radiosurgery plans. *Int J Radiat Oncol Biol Phys*, **57**(4): 1141-1149.
  18. Li T, Irmen P, Liu H, Shi W, Alonso-Basanta M, Zou W, et al. (2019) Dosimetric Performance and Planning/Delivery Efficiency of a Dual-Layer Stacked and Staggered MLC on Treating Multiple Small Targets: A Planning Study Based on Single-Isocenter Multi-Target Stereotactic Radiosurgery (SRS) to Brain Metastases. *Front Oncol*, **9**: 7.
  19. Yaparpalvi R, Garg MK, Shen J, Bodner WR, Mynampati DK, Gafar A, et al. (2018) Evaluating which plan quality metrics are appropriate for use in lung SBRT. *Br J Radiol*, **91**(1083): 20170393.
  20. Zhang J, Peng Y, Ding S, Zhu J, Liu Y, Chen M, et al. (2020) Comparison of Different Combinations of Irradiation Mode and Jaw Width in Helical Tomotherapy for Nasopharyngeal Carcinoma. *Front Oncol*, **10**: 598.

